

# Self-Organization of a Dichloromethane Droplet on the Surface of a Surfactant Containing Aqueous Solution

Florian Wodlei and Véronique Pimienta<sup>(✉)</sup>

IMRCP Laboratory, Paul Sabatier University, 118 Route de Narbonne,  
31062 Toulouse, France  
pimienta@chimie.ups-tlse.fr

**Abstract.** We investigate the dynamics of a dichloromethane droplet placed on the surface of an aqueous solutions of cetyltrimethylammonium bromide. By varying the surfactant concentration, we observe a rich variety of different shapes, ranging from pulsating over rotating to polygonal-like shaped drops, during the dissolution process. These remarkable shapes seem to be the result of the complex interplay between numerous processes including solubilization, evaporation, mass transfer and adsorption of the surfactants at the water/oil interface.

**Keywords:** Dichloromethane · Droplets · Cetyltrimethylammonium bromide (CTAB) · Dissolution · Evaporation · Mass transfer · Adsorption of surfactants · Marangoni instability

## 1 Introduction

Far-from-equilibrium systems show a great variety of spatial and temporal patterns, which are known as dissipative structures. The interplay between physico-chemical processes and mass or heat transfer can give rise to convective flows that may form such structures (Davies and Rideal 1963). The origin of dissipative structures, such as regular convective cells, interfacial deformations or interfacial turbulences, is often the conversion from chemical to mechanical energy (Eckert et al. 2012).

Specially the flows, which are triggered by density or surface tension gradients, are crucial to many natural phenomena, like ocean and atmospheric flows (Budroni et al. 2012). They are also crucial to processes like extraction, spreading of spills in aquifers or oil recovery and of course crucial to chemical reactors at all scales.

The energy transduction, that is created when the size of the phases in contact is very different, can give rise to spontaneous motion of the smaller phase (de Gennes et al. 2003). This is the case for liquid drops on solid or liquid surfaces (Zhao and Pumera 2012; Pimienta and Antoine 2014).

Symmetry breaking, which is inherent of motion, is obtained on solid surfaces by external constraints like thermal gradients or concentration gradients

of imprinted chemicals on the surface (Chaudhury and Whitesides 1992). On liquid surfaces motion can be induced spontaneously by the drop itself. Such autonomous behaviour is at the origin of the interest for such systems in relation with artificial cell design. There, by observing and mimicking the shapes and trajectories, which are spontaneously chosen in biological systems to adapt to motility (Bush and Hu 2006), the aim is to identify the energy sources that drive the different propulsion mechanisms. Motion is one of the vital functions of microorganisms in search of new resources.

The system of interest here is a drop of dichloromethane (DCM) deposited on a cetyltrimethylammonium bromide (CTAB) solution. By changing the surfactant concentration, which plays the role of a control parameter, the drop shows a succession of well defined, highly ordered patterns (Pimienta et al. 2011).

In the following, we will first go back to earlier observations, obtained under biphasic conditions, which have caused our interest for this system. In the second part of the article, we will describe the main regimes observed in the drop geometry.

## 2 Experimental Part

### 2.1 Biphasic System

Cetyltrimethylammonium bromide (CTAB) (Aldrich,  $\geq 99\%$ ), dichloromethane (DCM,  $\rho = 1.33 \text{ g} \cdot \text{cm}^{-3}$ ) (Aldrich, HPLC grade) aswell as ultra-pure water (resistivity  $\geq 18 \text{ M}\Omega \cdot \text{cm}$ ) for preparing the solutions were used. All chemical reagents used were of analytical grade.

Oscillations were recorded in a glass beaker with a 31 mm inner diameter without stirring. 15 mL of the organic solution (DCM) was placed at the bottom of the beaker. Then, 15 mL of aqueous solution containing CTAB was carefully placed on top of the organic phase.

Surface tension measurements were performed using a small cylinder (diameter 2.8 mm; 10 mm high) made of high-density polyethylene and connected to a microbalance (Fig. 1).

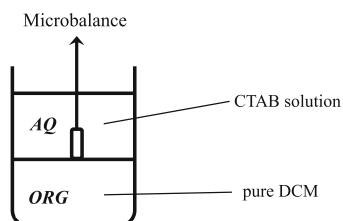


**Fig. 1.** Sketch of the setup for the system in the biphasic configuration in a 30 mL beaker.

## 2.2 Drop Configuration

The same reactants mentioned above were used for this configuration. 25 mL of the aqueous solution containing CTAB were poured in a Petri dish of 7 cm diameter. Then, a drop of 25  $\mu\text{L}$  of the organic solution (DCM) was placed carefully on the surface of the aqueous solution with a HPLC micro-syringe. After addition, the Petri dish was covered.

## 2.3 Visualization Techniques in the Drop Configuration

To visualize the droplet on the solution two techniques were used. The first, called *Shadowgraphy*, is realized by the illumination of the system from the top with a collimated light beam (a LED light source with fibre connection was used). Then, the projected shadow, that is produced by the highly curved regions at the corner of the droplet, is recorded. The images, which are shown in the overview of the different shape regimes (Fig. 11), were recorded in this way.

The other technique used, called *Schlieren technique*, allows a better contrast of the drop. To obtain this, a sharp edge was placed between a LED back-light illumination and a focusing lens, exactly at the focal point of the lens. This creates an intensity gradient on the recorded image. This density gradient can be varied by changing the distances and the form of the sharp edge (Fig. 2). In all other images shown in this work this techniques has been used.

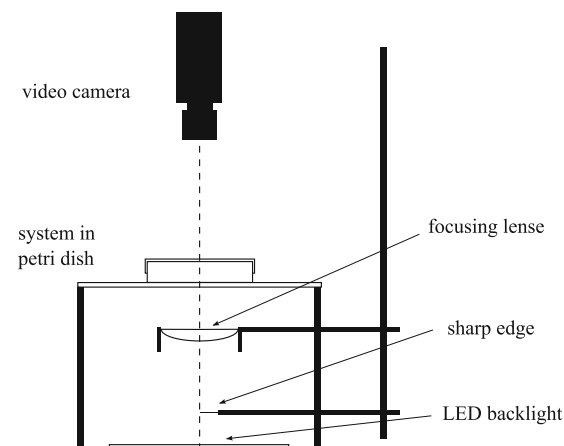


**Fig. 2.** Sketch of the optical setup for the Schlieren technique with the system in the drop configuration in the Petri dish.

## 3 Biphasic System

The first theoretical study aimed to establish criteria predicting Marangoni instability onset during solute mass transfer in biphasic systems was performed by

Sternling and Scriven (1959). They applied linear stability analysis to systems where a solute is transferred through a non-deformable interface between two semi-infinite liquid layers. The instability can develop in systems far from partition equilibrium and its appearance depends mainly on the solvent properties, the surface activity of the solute and on the formation of critical solute concentration gradients in the normal to the interface direction (Kovalchuk et al. 2012). Unstable transfer is expected when the solute diffuses out of the phase in which its diffusivity is lower and kinematic viscosity is higher.

The biphasic configuration of the present system, where, as described in the experimental part, an aqueous solution of CTAB is placed on the top of the heavier pure DCM phase fulfills the above criteria. The measured interfacial tension between the organic and the aqueous phase showed relaxation oscillations shown in Fig. 3 (Lavabre et al. 2005).

It was shown that these oscillations are induced by a periodic Marangoni instability. The decrease of the surface tension started just when movements at the interface were initiated (see vertical line in inset of Fig. 3).

The oscillations observed arise as a result of the mass transfer of CTAB (Fig. 3, B). Under mass transfer, concentration gradients build up in the diffusion layer (Pradines et al. 2007). The surfactant concentration in contact with the interface (that determines the corresponding adsorption level) decreases.

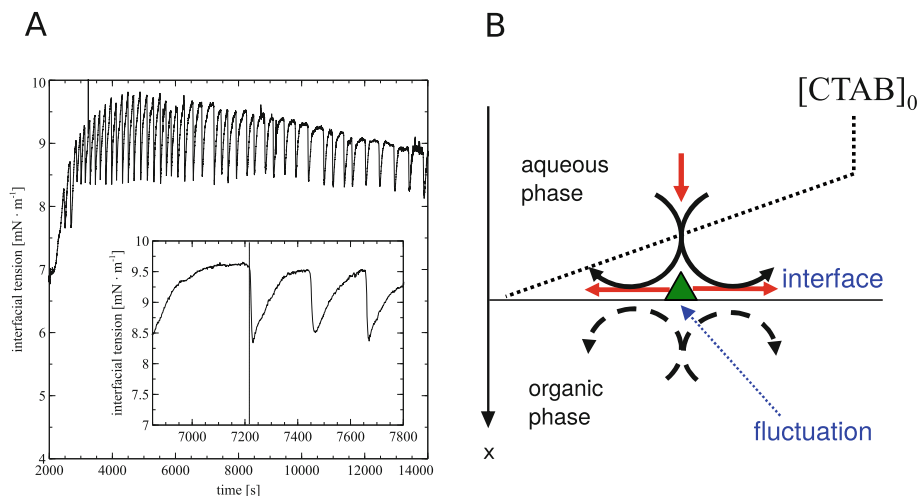


**Fig. 3.** A: oscillations of the interfacial tension between DCM and an aqueous solution containing 5 mM CTAB. Inset shows the oscillations between 6850–7800 sec in detail. The line in the inset indicates the time when movements at the interface were initiated. B: Schematic representation of the processes leading to oscillations in the biphasic system (details see text). Dashed line represents the normal to the interface concentration gradient of the surfactant, green triangle stands for the initial fluctuation, red arrows represent Marangoni flows and the curved arrows represent the convective cells induced by the Marangoni instability (Colour figure online)

At the interface, concentration heterogeneities are likely to occur, leading to tangential concentration gradients that induce stretching of the interface due to the Marangoni effect. This radial flow creates in turn a vertical flow that brings aqueous solution from the bulk, richer in surfactants, to the interface and will amplify the initial surface heterogeneities to give rise to convective flows in both phases. The related intense mixing of the aqueous layer near the interface destroys the normal gradients, the instability vanishes, and the system switches to a slower, diffusive process. During this phase, normal gradients, induced by CTAB mass transfer, built up again and the cycle starts anew.

## 4 Drop Configuration

In this configuration, where, as described in the experimental part, a drop of DCM is placed on the surface of an aqueous phase containing CTAB, there are other processes in addition to CTAB mass-transfer. Due to the low boiling point ( $T_{\text{bp}} = 39.6\text{ }^{\circ}\text{C}$  at 1 atm) and the partial miscibility of DCM (solubility in water is 0.15 M), evaporation and dissolution of DCM in the aqueous phase are also at play in this geometry.

The evolution of the drop shows two phases, an induction period, during which the drop shrinks while maintaining its circular shape, and a second phase at which the drop starts to deform in a self-organized manner before its final disappearance.

### 4.1 Induction Period

We measured the initial diameters of the deposited drop as a function of the CTAB concentration and observed the same trend as for the air/water interfacial tension (Fig. 4). Below the critical micellar concentration ( $\text{cmc} = 0.9\text{ mM}$ ),  $\gamma_{\text{w/a}}$  increases as does the initial diameter. After the cmc, both  $\gamma_{\text{w/a}}$  and the initial diameter remain constant.

If we assume a spherical cap geometry for the heavy DCM drop, the forces acting on the triple contact line can be represented by the Neumann triangle as shown in Fig. 5. The corresponding young equation reads  $\gamma_{\text{w/a}} = \gamma_{\text{o/a}} + \gamma_{\text{w/o}} \cdot \cos \theta$ .

A decrease of the water/air interfacial tension,  $\gamma_{\text{w/a}}$ , results in this case in a more compact drop (decreased diameter and increased contact angle), which is what we observe experimentally.

We have also measured the time span of the induction period for a  $25\text{ }\mu\text{L}$  DCM drop. For 0.25 mM and 0.5 mM, no induction time is observed, the unstable regime starts immediately. The longest induction period is observed at 1 mM, while its duration decreases again with increasing CTAB concentration.

In correlation to the variation of the initial diameter it appears that flatter drops (i.e. before the cmc) immediately enter the unstable regime while thicker drops need to reach a critical size before the instability is triggered. It looks as if the drop has to be small (flat) enough for the instability to start. In other words, surface tension forces need to overcome gravity effects in order to trigger the Marangoni instability.

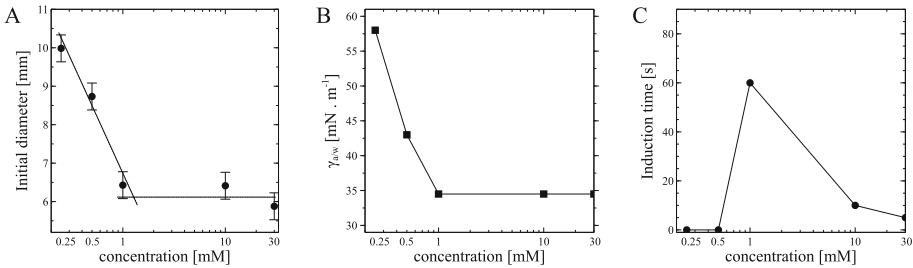


**Fig. 4.** Initial diameter (A), water/air interfacial tension (B) and induction time (C) as a function of the CTAB concentration.

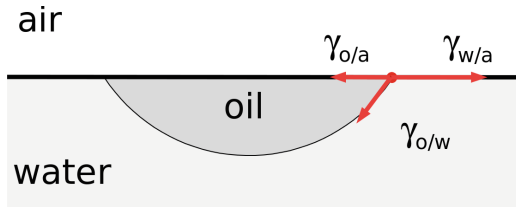


**Fig. 5.** Forces acting on a liquid droplet on a liquid surface in a spherical cap approximation according to the Young equation.

The decrease of the induction time for higher CTAB concentrations may be related to an increased solubilization rate due to the formation of CTAB swollen micelles (i.e. the formation of an oil in water microemulsion) (Tadmouri et al. 2008).

## 4.2 Pattern Formation - Marangoni Instability

**Spreading and Translation.** Examples of motions of drops on liquid surfaces are known in literature like the pentanol droplet of Nagai et al. (2005) or the aniline droplet of Chen et al. (2009), both on aqueous solutions. The aniline drop is similar to the present system in the sense that dissolution, evaporation and density effects are also involved. In this case evaporation and solubilization are relatively slow and the drop appears as a macroscopic drop coexisting with a surrounding precursor film. Two different kinds of motion are observed: bee-like motion and circular motion that could last for hours. Motility was ascribed to a surface tension imbalance at the front and rear of the drop. This difference, revealed by a difference in contact angle, was attributed to the precursor film. The film is driven by a Marangoni flow and may lose its initial symmetry (by fluctuations or induced manually). The initiated translation is then sustained by the dissymmetry of the surface active film pointing to the rear of the drop.

For the DMC drop on the CTAB solution, the film and its distortion are eye visible (Fig. 6). Motion is however observed only transiently, for 3 or 4 s (the whole process lasts for about 20 s). The main regime appears as a drop

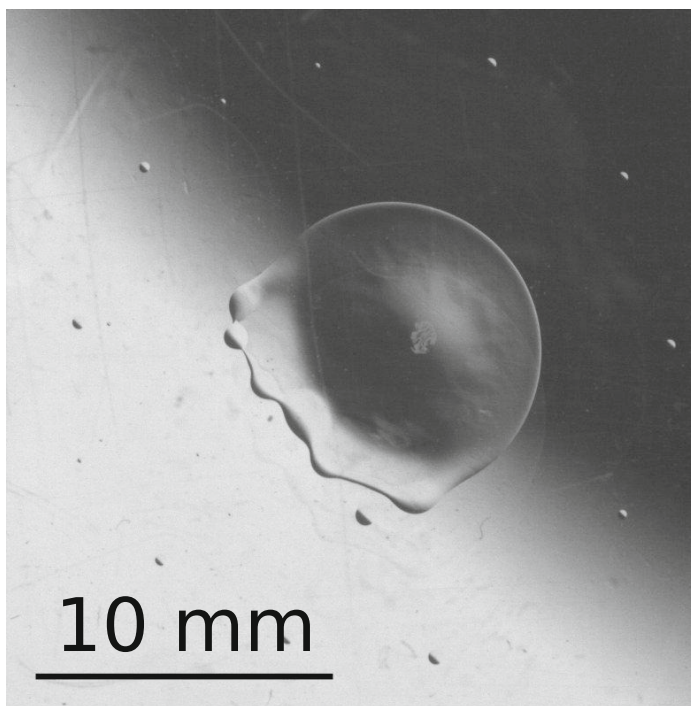


**Fig. 6.** Translation of a DCM drop on a 0.25 mM CTAB solution.

surrounded by a thin film terminated by a ring of smaller droplets. At some point, the film recoils on one side of the drop pushing the drop on the opposite side. Motion gets started by the induced dissymmetry. While the asymmetric shape is maintained, circular or translational motion are observed.

**Pulsations.** To our knowledge, there are two examples of similar pulsations in the literature. Bates et al. (2008) report on a pulsating regime, of a very short life time, that gives rise to the ejection of a ring of droplets for a 1-butanol drop cooled to 1 °C deposited on a 40 °C water phase. Another example is a mineral oil drop containing a non-ionic, non-water soluble surfactant placed on water, which is reported by Stocker and Bush (2007). The time scale here is longer (tens of seconds) but the recorded pulsations are very irregular compared to the one in the present system.

For a CTAB concentration of 0.5 mM, pulsations can last between 5 and 20 s with a mean frequency of about 1 Hz. Each pulsation consists of a rapid spreading of the drop. At maximum expansion, which represents close to 25 % of the initial drop radius, the rim formed at the edge of the expanding film undergoes a Rayleigh-Plateau-like instability and breaks up into small droplets that move radially away from the drop (over a distance of 5 to 6 mm) and rapidly disappear by evaporation and dissolution. After detachment of the rim the remaining film recedes to form a compact drop again (Fig. 7).

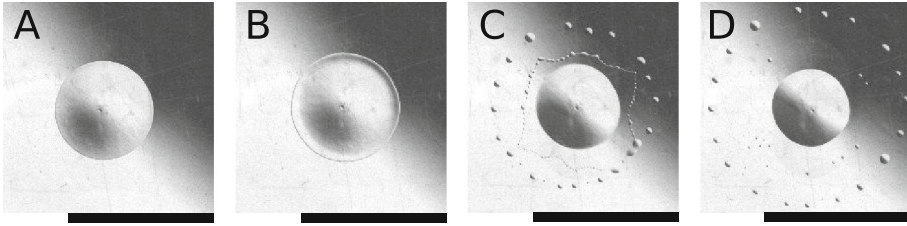


**Fig. 7.** Pulsating DCM drop on a 0.5 mM CTAB solution. A: Drop starts to expand ( $t = 0$  s). B: Rim is forming and expanding ( $t = 160$  ms). C: Rim breaks up in several droplets while the film between rim and droplet is receding ( $t = 345$  ms). D: Drop has ejected his rim completely and is about to start for another pulsation ( $t = 435$  ms). Black bar corresponds to 10 mm.

The regularity and conservation of the symmetry during the beating pattern are reflected in the time evolution of the drop radius (Fig. 8).

The recorded oscillations are not time-symmetric: the ascending, spreading parts are slightly longer ( $\sim 0.6$  s) than the descending, receding parts ( $\sim 0.4$  s). This time-asymmetry increases significantly in the course of time. By considering a very simple mechanical model of rim pulsations the time evolution of the drop radius can be perfectly reproduced (Antoine and Pimienta 2013).

The drop rim is described as a toroidal tube of oil, that is located at the drop radius position  $R(t)$ , having a (time-dependent) mass  $m$ . A time-dependent spring parameter  $k(t)$ , that takes all the springlike forces acting on the rim into account, is used. These forces are surface tensions, Marangoni stress, as well as the drop surface elasticity due to the surfactant monolayer. The spring parameter can be seen as the opposite of an effective spreading coefficient ( $S_{\text{eff}}(t) = -k(t)/2\pi$ ).

The model also takes into account the hydrostatic force acting on the rim and also a kind of damping force, that is caused by the friction of the toroidal rim. Finally, by summing up all forces, the dynamics of the rim is described by:

$$\frac{d}{dt} \left( m(t) \frac{dR}{dt} \right) = k(t)R + k_0 \frac{R_0^4}{R^3} - bR \frac{dR}{dt}$$

A constant mass  $m_0$  and a decreasing spring parameter  $k(t)$  is considered for the mean ascending part of  $R(t)$  and a constant spring parameter  $k_0$  and an increasing mass  $m(t)$  for the mean receding part. The whole curve of  $R(t)$  can be simulated by choosing a simple rim breakup criterion given by the capillary length. To account for the slight period increase observed, a slight increase of the rim mass over all of the pulsations is included.

In other words, the above scenario can be interpreted as follows: the oscillations are the result of Marangoni induced spreading due to a non homogeneous distribution of the CTAB at the water/oil interface. During expansion gradients are enhanced and spreading is amplified. This leads to a critical thickness of the film at the rear of the rim, which detaches while the film dewets to reform the initial drop.



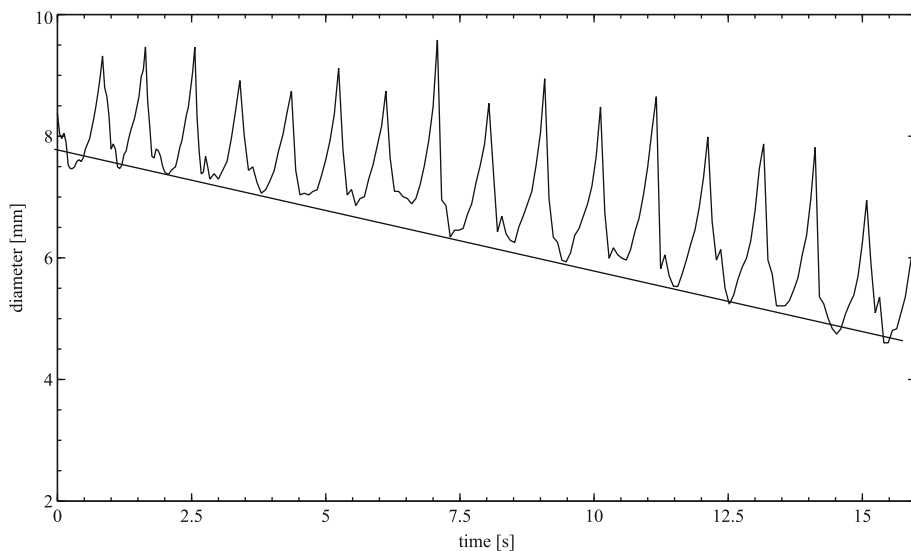


**Fig. 8.** Regular oscillations of the diameter of a pulsating DCM droplet on a 0.5 mM CTAB solution. The global linear decrease of the drop diameter can be attributed to the mass loss of the droplet.

**Rotation.** For a CTAB concentration of 10 mM, the drop undergoes a major shape deformation after the induction period, leading to an elongated structure with two sharp tips (Fig. 9). This structure then rotates in an arbitrary (clockwise and counterclockwise rotations are equally observed) but constant direction. The rotating two-armed drop is the most frequently encountered structure, but also rotating drops with three or sometimes four tips are observed.

Typically a drop can perform between 30 and 60 rotations with a steady rotation frequency of around 1.9 Hz, which is independent of the drop volume and time. During this stable rotation, the drop ejects smaller droplets from its tips. Each daughter droplet moves approximately 4 mm, flattens slightly, and then decays into several smaller droplets, that finally disappear.

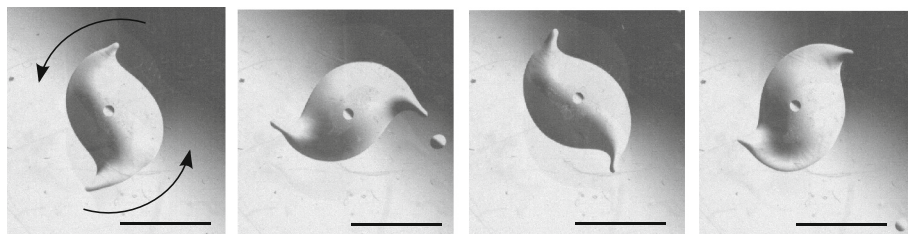


**Fig. 9.** Rotating of a DCM drop on a 10 mM CTAB solution (time increases from left to right). Approx. 1 rotation is shown (with 200 ms between each image). Black bar corresponds to 5 mm.

Although there are no examples of rotating drops in literature, there are rotating solids and gels on liquid phases (e.g. Nakata et al. 1997; Sharma et al. 2012).

In the article by Nakata et al. a solid camphor fragment with a comma-shaped form is rotating. The authors explain the rotation in the same way as the pure translation of the aniline drop, which is discussed above. The dissolving camphor forms a thin layer at the interface which locally reduces the interfacial tension. In the concave region of the “rotor”, due to the curvature, there is an accumulation of dissolved camphor in contrast to the convex region. Therefore a gradient in the surface tension is created and the rotor moves with the convex region ahead and the fragment starts to rotate.

For the DCM drop the same mechanism might be at play. Moreover the constant rotation frequency could be explained by the fact that the concentration in the concave regions of the rotors of the drop are continuously renewed from the bulk solution of the droplet, which is pure DCM.

**Polygonal-Like Shape.** For higher CTAB concentrations, a polygonal-like shape is observed (Fig. 10). After the induction period small tips form along the edge of the drop, which confers the drop the shape of a polygon. This tips move and when two of them collide they can give rise to the ejection of a smaller

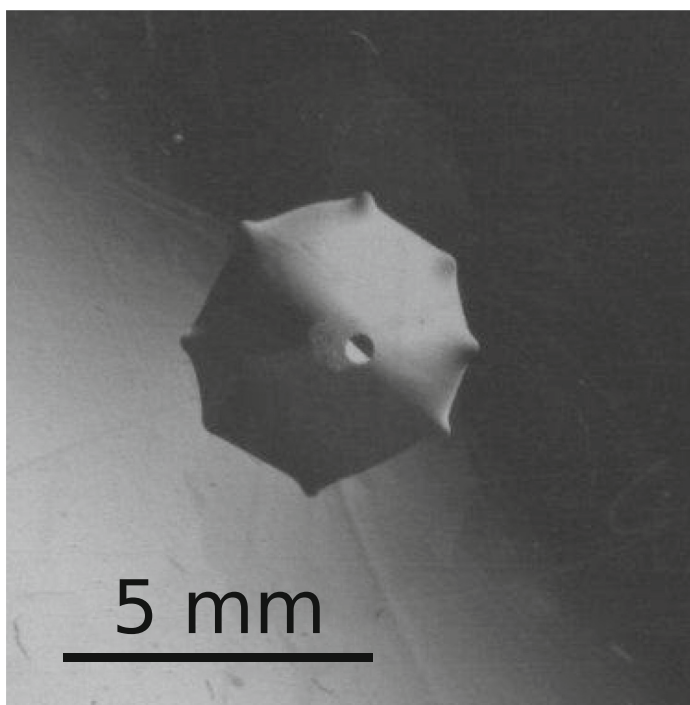


**Fig. 10.** Polygonal-like shaped drop on a 30 mM CTAB solution.

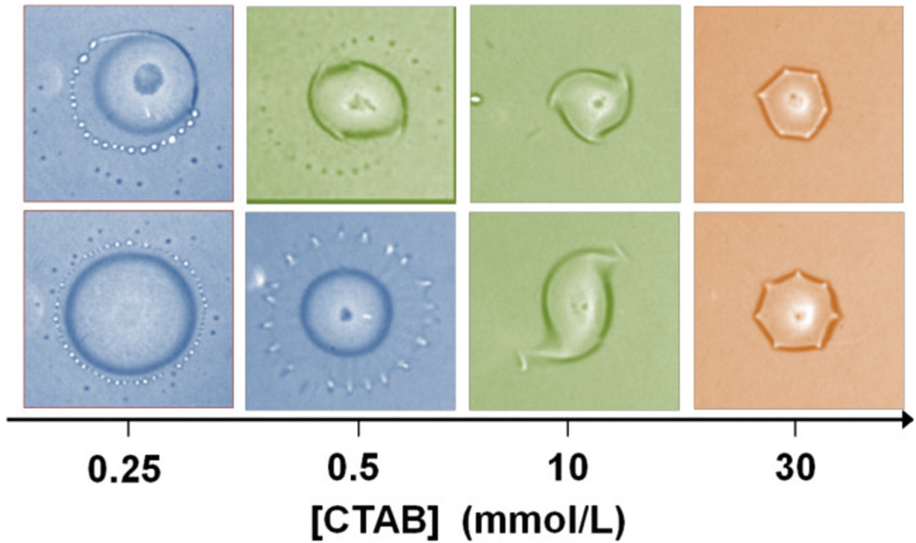


**Fig. 11.** Overview of the different regimes as a function of the CTAB concentration and time (vertical axis shows the time evolution).

droplet. During shrinkage of the drop the number of tips is reduced until the final disappearance of the drop. At the moment, we have no insight on this behaviour, which, to our knowledge, has never been described in the literature.

## 5 Conclusion and Perspectives

We described here the complex shape evolution of a DCM droplet on the surface of a CTAB containing aqueous solution. An overview of the different shape regimes is given in Fig. 11 as a function of the CTAB concentration. The phenomena observed range from spreading and dewetting below the cmc to rotating and polygonal-like shaped drops above the cmc.

The system described here is chemically extremely simple and easy to handle but gives rise to complex coupled physical processes. The surfactant concentration, used here as a control parameter, induces an amazing range of shapes and motion patterns. Coupled to these shape-forming processes is the emission of very small but macroscopic droplets. This system is the first example of such a sequence of highly ordered patterns induced by coupled hydrodynamic instabilities. The resulting structures show very efficient motility, internal agitation and dispersion properties.

We believe that this system for which the transitions between several regimes are driven by a controlled and progressive change of the physico-chemical properties, offers a great opportunity of a step forward in the understanding and modeling of fundamental knowledge in the very broad field of convective instabilities.

## References

- Antoine, C., Pimienta, V.: Mass-spring model of a self-pulsating drop. *Langmuir* **29**(48), 14935–14946 (2013)
- Bates, C.M., Stevens, F., Langford, S.C., Dickinson, J.T.: Motion and dissolution of drops of sparingly soluble alcohols on water. *Langmuir* **24**, 7193–7199 (2008)
- Budroni, M.A., Rongy, L., De Wit, A.: Dynamics due to combined buoyancy- and Marangoni-driven convective flows around autocatalytic fronts. *Phys. Chem. Chem. Phys.* **14**, 14619–14629 (2012)
- Bush, J.W.M., Hu, D.L.: Walking on water: biolocomotion at the interface. *Annu. Rev. Fluid Mech.* **38**, 339–369 (2006)
- Chaudhury, M.K., Whitesides, G.M.: How to make water run uphill. *Science* **256**(5063), 1539–1541 (1992)
- Chen, Y.-J., Nagamine, Y., Yoshikawa, K.: Self-propelled motion of a droplet induced by marangoni-driven spreading. *Phys. Rev. E* **80**, 016303 (2009)
- Davies, J.T., Rideal, E.K.: *Interfacial Phenomena*. Academic Press, New York (1963)
- de Gennes, P.-G., Brochard-Wyart, F., Quere, D.: *Capillarity and Wetting Phenomena: Drops, Bubbles, Pearls, Waves*. Springer, New York (2003)
- Eckert, K., Acker, M., Tadmouri, R., Pimienta, V.: Chemo-Marangoni convection driven by an interfacial reaction: pattern formation and kinetics. *Chaos* **22**(3), 037112 (2012)
- Kovalchuk, N.M., Pimienta, V., Tadmouri, R., Miller, R., Vollhardt, D.: Ionic strength and pH as control parameters for spontaneous surface oscillations. *Langmuir* **28**(17), 6893–6901 (2012)
- Lavabre, D., Pradines, V., Micheau, J.C., Pimienta, V.: Periodic Marangoni instability in surfactant (CTAB) liquid/liquid mass transfer. *J. Phys. Chem. B* **109**(15), 7582–7586 (2005)
- Nagai, K., Sumino, Y., Kitahata, H., Yoshikawa, K.: Mode selection in the spontaneous motion of an alcohol droplet. *Phys. Rev. E Stat. Nonlin. Soft Matter Phys.* **71**(6 Pt 2), 065301 (2005)
- Nakata, S., Iguchi, Y., Ose, S., Kuboyama, M., Ishii, T., Yoshikawa, K.: Self-rotation of a camphor scraping on water: new insight into the old problem. *Langmuir* **13**(16), 4454–4458 (1997)
- Pimienta, V., Antoine, C.: Self-propulsion on liquid surfaces. *Curr. Opin. Colloid Interface Sci.* **19**, 290–299 (2014)
- Pimienta, V., Brost, M., Kovalchuk, N., Bresch, S., Steinbock, O.: Complex shapes and dynamics of dissolving drops of dichloromethane. *Angew. Chem. Int. Ed.* **50**, 10728–10731 (2011)
- Pradines, V., Tadmouri, R., Lavabre, D., Micheau, J.C., Pimienta, V.: Association, partition, and surface activity in biphasic systems displaying relaxation oscillations. *Langmuir* **23**, 11664–11672 (2007)
- Sharma, R., Chang, S.T., Velez, O.D.: Gel-based self-propelling particles get programmed to dance. *Langmuir* **28**(26), 10128–10135 (2012)
- Sternling, C.V., Scriven, L.E.: Interfacial turbulence: hydrodynamic instability and the marangoni effect. *AIChE J.* **5**, 514–523 (1959)
- Stocker, R., Bush, J.W.M.: Spontaneous oscillations of a sessile lens. *J. Fluid Mech.* **583**, 465–475 (2007)
- Tadmouri, R., Zedde, C., Routaboul, C., Micheau, J.C., Pimienta, V.: Partition and water/oil adsorption of some surfactants. *J. Phys. Chem. B* **112**(39), 12318–12325 (2008)
- Zhao, G., Pumera, M.: Macroscopic self-propelled objects. *Chem. Asian J.* **7**, 1994–2002 (2012)